

RESEARCH ARTICLE

Experimental and numerical study of cold-formed steel beams with web perforations

Casim Yazıcı^{1*}, Muhammed Gürbüz²

- Dogubayazit Ahmedi Hani Vocational School, Ağrı İbrahim Çeçen University, Ağrı, Türkiye
- ² Department of Civil Engineering, Erzurum Technical University, Erzurum, Türkiye

Article History

Received 18 June 2024 Accepted 5 September 2024

Keywords

Cold-formed steel beams Web perforations Shear performance Finite element analysis Structural behavior

Abstract

This study focuses on the experimental and numerical investigation of cold-formed steel (CFS) beams with web perforations to assess their shear performance. Twelve samples were tested, all processed from high-strength, cold-formed steel sheets of grade S235 with a thickness of 1.5 mm. The specimens, designated as CC, were formed by interlocking two C-sections and welded together. Various parameters were analyzed, such as the shear-span ratio, hole depth-to-web height ratio (dh/h), and web height-to-thickness ratio. The experimental setup involved mid-span singlepoint loading conditions to evaluate the mechanical behavior of the beams. Circular holes with different diameters were strategically placed at the mid-height of the webs in two shear zones. The experimental results were validated using finite element analysis (FEA) conducted in ANSYS, ensuring the accuracy of the finite element model. The findings indicate that the ultimate bearing capacity of the specimens decreases as the hole depth-to-web height ratio increases. When the hole depth-toweb height ratio was small $(dh/h \le 0.4)$, the load-deflection curves declined rapidly after reaching the peak. Conversely, for a ratio of 0.5, the curves declined more gradually. Additionally, mid-span deflection decreased as dh/h increased, with significant variation observed for smaller ratios and stabilization for a ratio of 0.5. This research provides a comprehensive understanding of the shear behavior of coldformed steel beams with web openings. It offers valuable insights into the design and optimization of these structures, contributing to the safe and efficient application of CFS beams in various engineering contexts.

1. Introduction

Cold-formed steel (CFS) structures have garnered significant attention due to their advantageous properties, such as high strength-to-weight ratio, ease of fabrication, and cost-effectiveness, making them an attractive option for various structural applications, including residential buildings, storage racks, and industrial facilities. One critical aspect of CFS structures is their ability to incorporate web openings, which facilitate the passage of utilities and reduce material usage, thereby enhancing structural efficiency [1].

However, the presence of web openings in cold-formed steel beams introduces complexities in their structural behavior. Specifically, web openings can significantly affect the shear and bending performance

eISSN 2630-5763 © 2023 Authors. Publishing services by golden light publishing®.

^{*} Corresponding author (cyazici@agri.edu.tr)

of CFS beams, potentially reducing load-carrying capacity and altering failure modes. Consequently, understanding the influence of web openings on the structural performance of CFS beams is essential for their safe and efficient design [2].

Keerthan and Mahendran [3] highlighted that cold-formed steel elements are increasingly used as primary structural elements in construction industries worldwide due to the availability of thin, high-strength steel and advanced cold-forming technologies. Cold-formed lipped channel beams (LCBs) are commonly used as bending elements, such as floor beams and joists. However, their shear capacities are determined by limited design rules. The current practice in floor systems involves placing openings in the web of floor beams or joists to accommodate building services. The shear behavior of LCBs with web openings is complex, and their shear strengths are significantly reduced due to the presence of web openings. Limited research exists on the shear behavior and strength of LCBs with web openings, necessitating a detailed experimental study of 40 shear tests to investigate the shear behavior and strength of LCBs with web openings. Simply supported test specimens of LCBs with aspect ratios of 1.0 and 1.5 were loaded at mid-span until failure. The study presented the experimental results, finite element modeling of LCBs with circular web openings, and the development of improved shear design rules to investigate the mechanical behavior of cold-formed lipped 2C-section steel beams with various sizes of web openings under predominant shear effects. Thus, twelve groups of cold-formed 2C-section steel beams with web openings were tested under mid-span single-point loading conditions. Subsequently, a finite element model was developed using ANSYS, and the experimental results were compared with the FEA results to validate the accuracy of the finite element model. Through comprehensive testing, including specimens with a hole depth-to-web height ratio $dh/h \ge 0.5$ and finite element analysis, this study aims to provide a foundational basis for designing shear-carrying capacity in cold-formed steel beams with web openings [3].

Wang and Young [4] investigated the bending behavior of cold-formed steel elements with circular holes in the web, focusing on their ultimate moment capacities and failure modes. A total of 43 beams with different hole diameters and 10 section sizes were tested under four-point bending. The built-up sections were assembled using smart screws from two plain or lipped channels. The tests observed reductions in moment capacities and local buckling due to the presence of holes in the web plates of the beams. When the hole diameter-to-web depth ratio (*dh/hw*) was 0.5, the holes' effect on the beams' moment capacities was minimal. They extended the existing Direct Strength Method (DSM) to design cold-formed steel structural sections with holes. The predicted design strengths of DSM were compared with the test results, showing that the DSM formulas could predict the design strengths of perforated cold-formed open and closed section beams using the critical elastic local and distortional buckling moments, including the effects of the holes as proposed in the standards.

Pham et al. [5,6] proposed a new test device to reduce the impact of the bending moment on the shear carrying capacity of sections with relatively large shear opening ratios and recalibrated the existing North American Specification DSM design formulas. They introduced a dual-actuator test rig with two independently acting actuators at customizable displacement rates to control and minimize the applied bending moments in shear openings. Thus, shear strength close to the pure shear capacity can be achieved even at an aspect ratio of 2.0. The test results were combined with other available experimental data and used to validate and recalibrate the DSM design formulas included in the AISI S100:2016 Specification and AS/NZS 4600:2018 Standard.

Degtyareva et al. [7-12] presented finite element models and experimental studies of cold-formed steel channels with web openings subjected to shear. The models were developed in ANSYS and validated against test data. The effects of boundary conditions on the elastic shear buckling load and ultimate shear strength were numerically investigated using models with realistic boundary conditions and test setups. The results showed that boundary conditions affected the elastic shear buckling loads and ultimate shear strengths of

perforated channels more significantly than solid channels. They conducted extensive parametric analyses on the shear performance of CFS beams with perforated sections, including web perforation models. Temporary design equations were proposed for the shear capacity of CFS beams with web holes, considering channel flange width, flange lip length, and the overall design and application of such elements.

Thirunavukkarasu et al. [13] noted that cold-formed steel elements are often perforated with elongated web openings in practice to provide greater access to building service systems. Such elongated web holes in elements subjected to high shear forces affect their shear buckling characteristics and failure modes and generally reduce shear capacity. To better understand the shear behavior of cold-formed elements with elongated web sections, this study presents a numerical investigation using finite element method (FEM) models in ABAQUS/Standard to investigate the elastic shear buckling and post-buckling behavior of thinwalled channel sections. A fully nonlinear FEM model was developed and calibrated against previous shear tests on elements with elongated web holes using a dual actuator test rig. Based on the successful calibration of these tests, a parametric study was conducted to expand the resulting database.

CFS sections offer many design and construction advantages, including lightness and a high strength-toweight ratio. The SupaCee section was introduced to the CFS industry for its cost-effectiveness, increased strength, better structural performance, and high stiffness. The introduction of SupaCee sections led to investigations of their web discontinuities, buckling, and shear behavior. However, the structural behavior of SupaCee sections with web openings has not been addressed. Therefore, this study aims to analyze the shear behavior of SupaCee sections with web openings. The results of previous shear tests on SupaCee sections and lipped channel beam (LCB) sections with openings were validated using developed FE models. An extensive parametric study was conducted considering various geometric parameters such as depth, yield strength, thickness, and web opening ratios. Detailed study results indicated that existing design equations were overly conservative, leading to the proposal of new design equations with reduction factors to predict the ultimate shear capacity of SupaCee sections with web openings. Additionally, the shear capacities of SupaCee sections were compared with those of similarly sized LCB sections. Considering the availability of web openings to accommodate services and the ability of plain LCB sections to regain shear capacity, a web opening ratio of 0.2 is recommended. Based on the test results, finite element analysis was conducted on two new types of cold-formed steel beams with web openings, and relevant design formulas for the shear capacity of these elements were proposed [14,15].

Understanding the structural behavior of cold-formed steel beams with web openings is critical for the safe and efficient design of these systems. This study aims to bridge the gap between experimental observations and numerical predictions, providing a robust framework for evaluating and optimizing the performance of perforated cold-formed steel beams. The findings from this research will offer valuable guidance for the practical application of these members in various engineering contexts [16].

The use of cold-formed steel (CFS) members has increased significantly in recent years due to their numerous benefits, such as structural efficiency, cost-effectiveness, and ease of installation for electrical and plumbing systems. These installations often require web holes in the steel members, which can affect their structural integrity. This study reviews the existing literature on the behavior of CFS members with web holes, focusing on experimental and numerical research conducted primarily over the past 15 years. The research encompasses the impact of web holes on CFS members under various stress conditions, including compression, bending, web crippling, and shear. Notably, most progress in this area has been achieved in the past decade, with significant advancements in understanding how web holes influence buckling modes and ultimate strength. The review also covers design proposals and methods, highlighting the main concepts from principal design codes such as the North American (AISI S100), European (EN 1993-1-3), Australian/New Zealand (AS/NZS 4600), and Chinese (GB 50018) standards. This comprehensive review identifies existing research gaps and suggests future study directions. It aims to consolidate the current knowledge of CFS

members with web holes, providing a valuable resource for structural engineers and researchers. Key findings include the necessity for specific design guidelines to account for web holes, the importance of considering local and distortional buckling modes, and the effectiveness of various numerical methods for predicting the behavior of perforated CFS members. Overall, this paper underscores the need for ongoing research to refine design methods and enhance the safety and performance of CFS structures with web holes, ensuring their reliable application in modern construction practices [17].

Cold-formed steel elements often feature various numbers and shapes of web openings in engineering applications to facilitate the installation of electrical and mechanical systems. These openings increase usable space and floor height by allowing utilities to pass through them. Previous studies have examined the behavior of cold-formed steel elements with web openings. Recent research has focused on the bending capacity of cold-formed steel beams, with limited attention to the shear performance of cold-formed C-section beams with web openings.

While previous studies have examined various aspects of cold-formed steel elements with web openings, there remains a gap in our understanding of the shear performance of cold-formed C-section beams with web openings, particularly for hole depth-to-web height ratios $(dh/h) \ge 0.5$. This study aims to bridge this gap by providing a comprehensive experimental and numerical investigation of the shear behavior of cold-formed steel beams with web perforations. The originality of this research lies in its focus on a wide range of hole depth-to-web height ratios (0 to 0.5) and its detailed analysis of the interaction between shear-span ratio, hole size, and web height-to-thickness ratio.

A key novelty of this study is the use of a CC section formed by interlocking two C-sections, which differs from the conventional single C-sections or back-to-back C-sections commonly found in the literature. This innovative section design allows for improved stability and load-bearing capacity, potentially offering new insights into the behavior of cold-formed steel beams with web openings.

The purpose of this study is twofold: (1) to experimentally determine the effects of web openings on the ultimate bearing capacity, failure modes, and load-deflection characteristics of cold-formed steel beams with this novel CC section, and (2) to develop and validate a finite element model that can predict the shear behavior of these beams. The scope of this research encompasses twelve test specimens with varying hole sizes, subjected to mid-span single-point loading conditions. By combining experimental results with finite element analysis, this study aims to provide valuable insights for the design and optimization of cold-formed steel beams with web openings, contributing to their safe and efficient application in various engineering contexts.

2. Experimental investigation

2.1. Test specimens

In this study, 12 samples were tested, all processed from high-strength, cold-formed steel sheets of grade S235 with a thickness of 1.5 mm. The specimens, designated as CC, were formed by interlocking two C-sections. These sections were welded every 70 cm with 1 cm welds. The details of the CC section formed by the combination of C-sections are shown in Fig. 1, while the details of a single C-section are provided in Fig. 1a. All dimensions of the specimens were defined based on the outer profile, as shown in Fig. 1b, where the nominal height of the web (h) was 120 mm. The nominal width of the flange (bf) was 50 mm, and the nominal width of the lip (bl) was 13 mm. The nominal thickness (t) of all test specimens was 1.5 mm. The meaning of the specimen labels is illustrated in Fig. 1c, where the T mark at the end of some labels indicates repeated specimens. Circular holes of different diameters were placed at the mid-height of the webs in two shear zones, as shown in Fig. 4. The ratio of the diameter of the circular hole to the web height (dh/h), i.e., the ratio

of hole depth to web height, varied from 0 to 0.5, with the sectional views provided in Fig. 2. The details of the beam specimens are provided in Table 1.

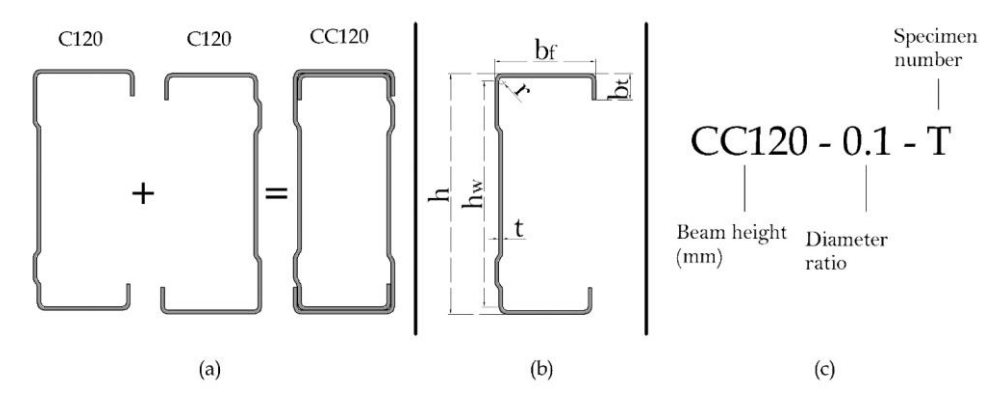


Fig. 1. (a) Combination of two C120 sections to form a CC120 section, (b) dimensions of CC120 section, and (c) specimen designation

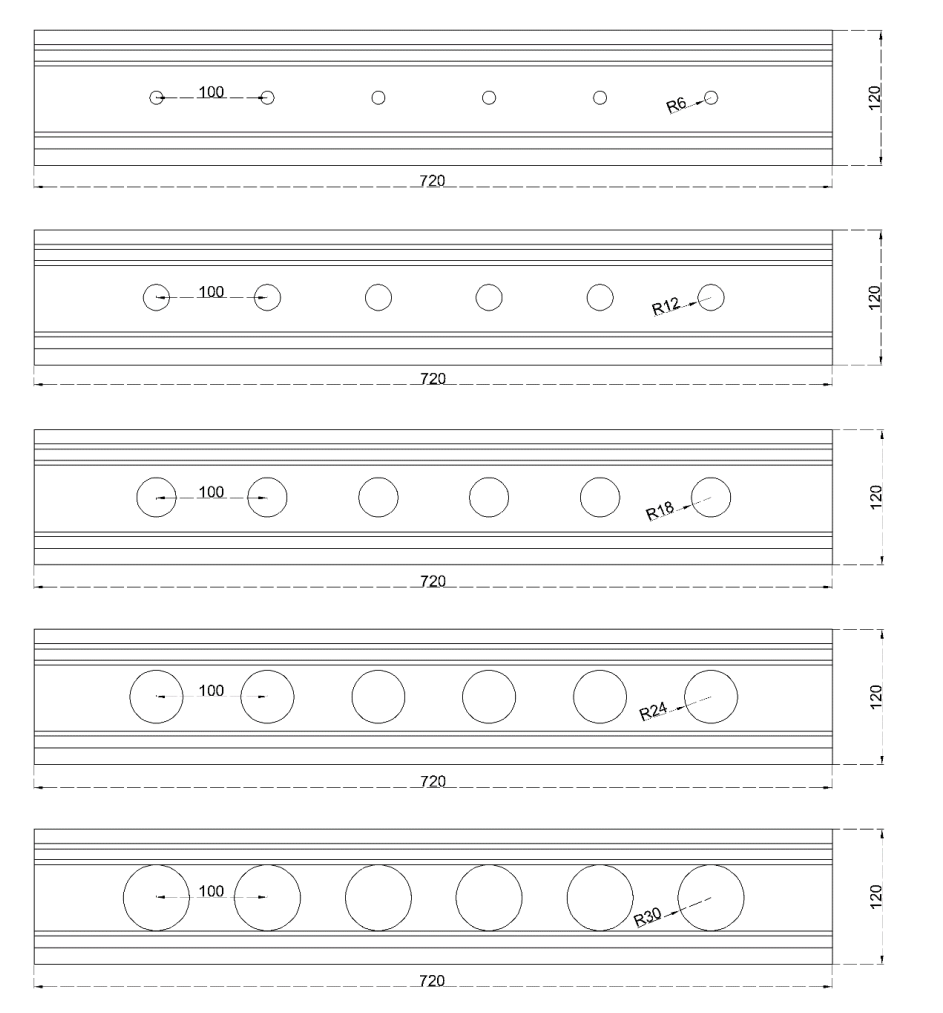


Fig. 2. Sectional views with circular specimens

Table 1. Details of the specimens

Specimen .	Web	Flange	Lip	Thickness	Hole	The hole depth-to-web height ratio	The shear-span ratio
	hw	bf	bl	t	dh	dh/h	a/h
CC120-0	112	50	13	1.5	0	0	0.83
CC120-0.1	112	50	13	1.5	12	0.1	0.83
CC120-0.2	112	50	13	1.5	24	0.2	0.83
CC120-0.3	112	50	13	1.5	36	0.3	0.83
CC120-0.4	112	50	13	1.5	48	0.4	0.83
CC120-0.5	112	50	13	1.5	60	0.5	0.83

2.2. Material characteristics

The beams utilized in this study were fabricated using the cold-forming method from steel plates. Tensile tests were carried out to determine the mechanical properties of the beam materials. These tests were performed according to ASTM E8/E8M-22 standards. Each group consisted of three specimens, ensuring reliable results. The tensile tests were carried out on a machine with a 250 kN capacity. The loading speed was 2.5 mm/min to maintain consistent testing conditions. The geometric specifications of the tensile coupon specimens and tensile test results are illustrated in Fig. 3, while the average mechanical properties derived from these tests are summarized in Table 2.

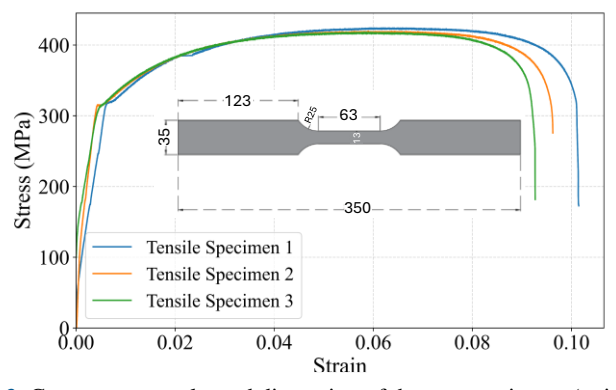


Fig. 3. Coupon test results and dimension of the test specimens (units in mm)

Table 2. Material properties of the test specimens

Member	Young's modulus, E (GPa)	Poisson's ratio, v	Thickness, t (mm)	Yield strength, Fy (MPa)	Ultimate strength, Fu (MPa)
				328	420
Beam	210	0.3	1.5	324	430
				332	413
			Average	328	421

2.3. Test method

2.3.1. Loading device

The single-point loading method was adopted for the test, and the concentrated load was applied to the middle load connector of the beam specimen. Round bars were used at both ends of the specimen to simulate a sliding hinge support. The testing setup is shown in Fig. 4. The longitudinal loading of the specimen was allowed to be free along its length without restricting its displacement.

3. Finite element model investigation

A commercial finite element software, ANSYS, was utilized to create the finite element model. A comparative analysis and verification against the test results were conducted to ensure the model's accuracy. This process confirmed that the model reliably represented the physical tests. Due to the symmetrical loading mode used in the test, the entire specimen was simplified.

In the meshing of the elements, hexahedral elements were not preferred due to gaps and curvilinear parts, and tetrahedral (Tet10 – SOLID187) elements were used by applying the patch-conforming method. The SOLID187 element is well suited to modeling irregular meshes and is defined by 10 nodes with three degrees of freedom at each node.

In the test, round bars simulated the sliding hinge support at both beam ends. The specimen's displacement along its length was not constrained, and no round bar was at the loading point. Stiffening plates were placed on one side of the web at the beam's ends and mid-span, connected by bolts to the load connector. Thus, the simplified model's boundary conditions were set as follows: at the beam ends, a point below the web section at the support was the coupling point, constrained with U1 = U2 = UR3 = 0. At the mid-span section, a point at the upper end of the web (the loaded part) was the coupling point, constrained with U3 = UR2 = UR3 = 0. In the test, the jack applied load uniformly to the load connector, transferring it to the beam. For the model, the displacement-loading method was used for finite element simulation, with a certain deflection along the Y direction applied at the mid-span coupling point. The analysis details are shown in Fig. 5. To verify the accuracy of the finite element model, the simulation analysis results were compared with the test results in terms of failure mode, ultimate bearing capacity, and load-deflection curve.

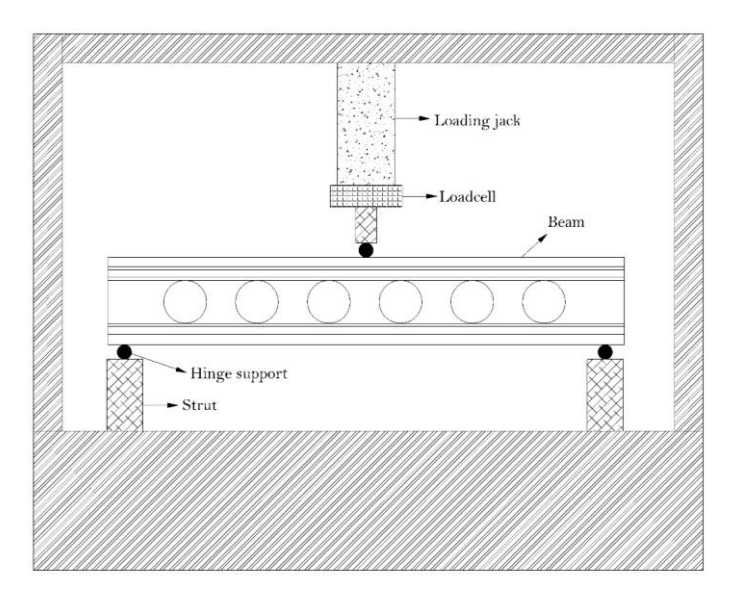


Fig. 4. Test frame system

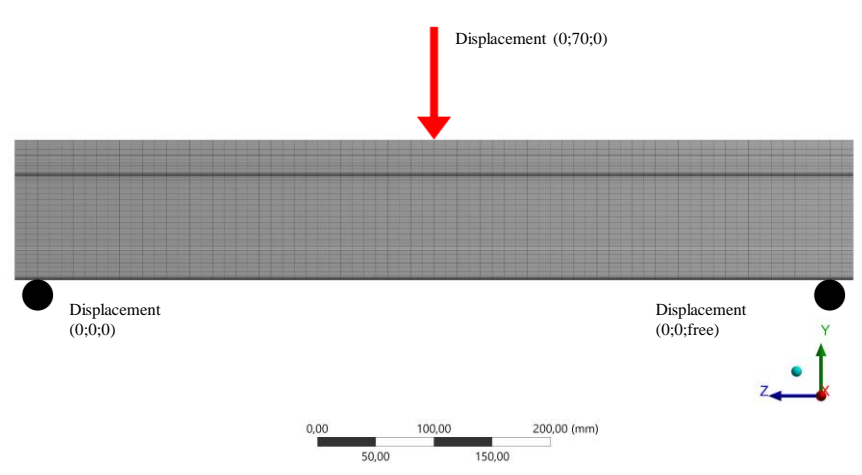


Fig. 5. Boundary conditions

4. Test results and discussion

4.1. Load-deflection curves

Given that the two joined C-sections in the test exhibited the same stress distribution and essentially similar displacements, a series of load-deflection curves for specimen CC120 are presented in Fig. 6. The experimental and analysis results' load-deflection curves are also included in Fig. 5. From the curves, it can be observed that under the same shear-span ratio, meaning with the same beam length, the ultimate bearing capacity of the specimens gradually decreased as the hole depth-to-web height ratio increased. When the hole depth-to-web height ratio was small ($dh/h \le 0.4$), the load-deflection curves at mid-span decreased rapidly after reaching the peak point. Conversely, when the hole depth-to-web height ratio was equal to 0.5 (dh/h = 0.5), the curves gradually decreased after reaching the peak point. Additionally, when the load reached the ultimate value, the corresponding deflection of the specimens varied with the hole depth-to-web height ratio. As the hole depth-to-web height ratio of specimens with the same length increased, the corresponding mid-span deflection gradually decreased when the load reached the ultimate value. When the hole depth-to-web height ratio was small ($dh/h \le 0.4$), the mid-span deflection of specimens with different hole sizes varied significantly upon reaching the ultimate load. This may be attributed to the failure modes of these specimens transitioning from dominant bending failure (local and distortional) to a combination of bending and shear failure. However, when the hole depth-to-web height ratio was equal to 0.5 (dh/h = 0.5), the mid-span deflection of specimens with different hole sizes varied slightly at the ultimate load, and the curves tended to stabilize.

As observed in Fig. 6, the load-displacement curves exhibit distinct behaviors for different hole depth-to-web height ratios (dh/h). For specimens with smaller ratios $(dh/h \le 0.3)$, the curves show a more pronounced peak followed by a relatively rapid decrease in load capacity. As the ratio increases $(dh/h \ge 0.4)$, the curves become more rounded at the peak, with a more gradual decrease in load capacity post-peak. This transition in behavior reflects a shift in the dominant failure mode from local buckling to a more distributed shear failure as the hole size increases. The sudden decreases observed in the load-displacement curves can be attributed to the onset of local buckling in the compression flange and web. As the load increases, stress concentrations develop around the web openings, leading to localized buckling. When this buckling occurs, there's a rapid loss of stiffness, resulting in a sharp drop in the load-carrying capacity.

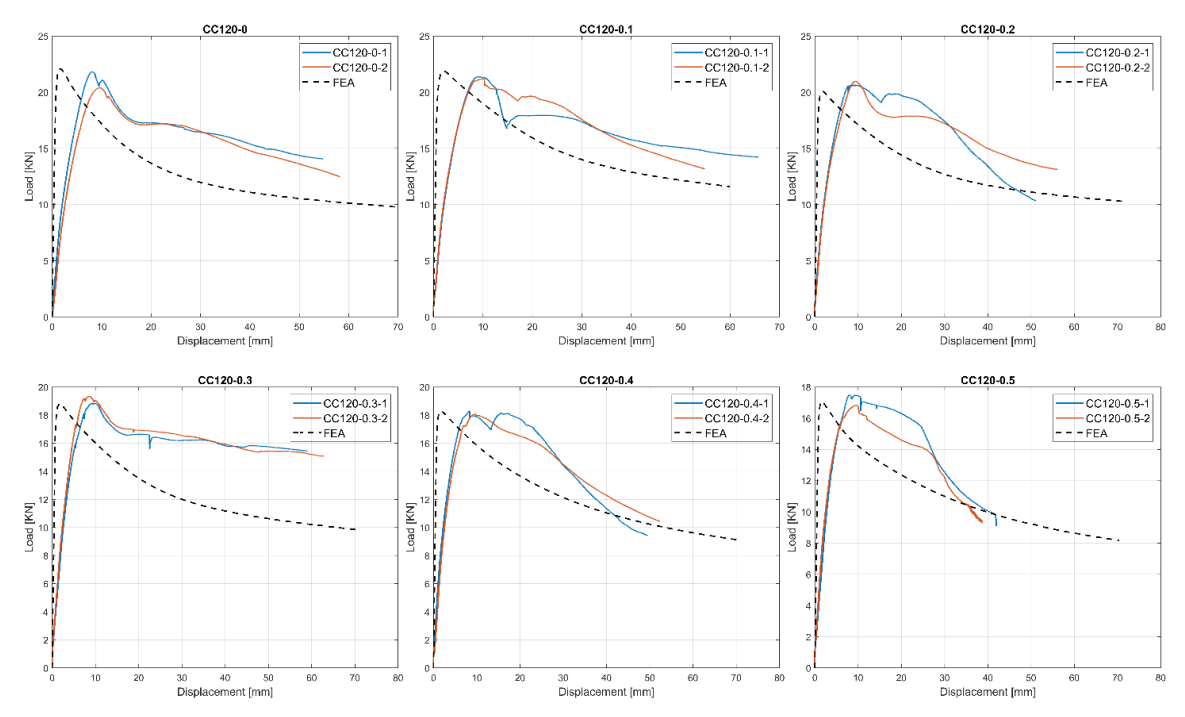


Fig. 6. The load-deflection curves at the mid-span of the specimens

There are notable differences between the experimental and FEA results, particularly in the post-peak region. While the FEA generally predicts the peak load with reasonable accuracy, it tends to overestimate the post-peak strength for specimens with smaller hole sizes $(dh/h \le 0.3)$. For larger hole sizes $(dh/h \ge 0.4)$, the FEA shows better agreement with experimental results in both peak load and post-peak behavior mechanisms, particularly the sudden loss of strength observed in some experimental cases. The FEA's prediction of initial structural stiffness varies in accuracy across the specimens. This initial structural stiffness, while related to the material's elastic properties, also incorporates the effects of beam geometry and web openings. The discrepancies between FEA and experimental results in this initial region suggest that the model may not fully capture all factors influencing the beam's initial structural response, particularly for specimens with smaller web openings.

4.2. Failure modes

It is found that the failure mode varies with changes in the shear-span ratio and hole size. In the same group of tests, the stress distribution and failure mode of specimens are consistent, so the results in the table are all the test results of specimen CC120. The failure mode for each specimen is presented in Fig. 7.

For the specimen with dh/h = 0, when the loading value is about 88% of the ultimate load, there is no obvious buckling deformation; at about 94% of the ultimate load, local buckling begins on the compression flange; at about 99% of the ultimate load, insignificant distortional buckling occurs near the mid-span; at the ultimate load, the failure modes include local buckling in the compression flange and coupling failure of insignificant distortional buckling.

For the specimen with dh/h = 0.1, at about 74% of the ultimate load, shear buckling begins in the web; at about 76% of the ultimate load, local buckling occurs in the compression flange near mid-span; at about 88% of the ultimate load, local buckling occurs in the compression flange, accompanied by insignificant distortional buckling; at the ultimate load, the failure modes include coupling shear failure in the web, local buckling in the compression flange, and insignificant distortional buckling.

For specimens with dh/h = 0.2 and dh/h = 0.3, shear buckling begins in the web at about 77% and 75% of the ultimate load, respectively; at about 89% and 85% of the ultimate load, insignificant distortional buckling occurs; at the ultimate load, the failure modes include coupling shear buckling failure in the web and insignificant distortional buckling in the compression flange.

For specimens with dh/h = 0.4 and dh/h = 0.5, due to larger hole sizes, shear buckling in the web occurs earlier and continues with loading; at about 85% of the ultimate load, the load-deflection curve enters the nonlinear stage; at the ultimate load, shear failure mainly occurs in the web.

When the web height-to-thickness ratio is constant and the shear-span ratio (a/h) is 1, the web is subjected to shear buckling at the ultimate load regardless of the hole size. When $dh/h \le 0.2$, coupling failure of local buckling in the compression flange and shear buckling in the web occur at the mid-span of the perforated specimen, accompanied by insignificant distortional buckling. When $dh/h \ge 0.3$, the specimen mainly experiences web shear failure. The comparative analysis of experimental and numerical failure modes is presented in Fig. 7.

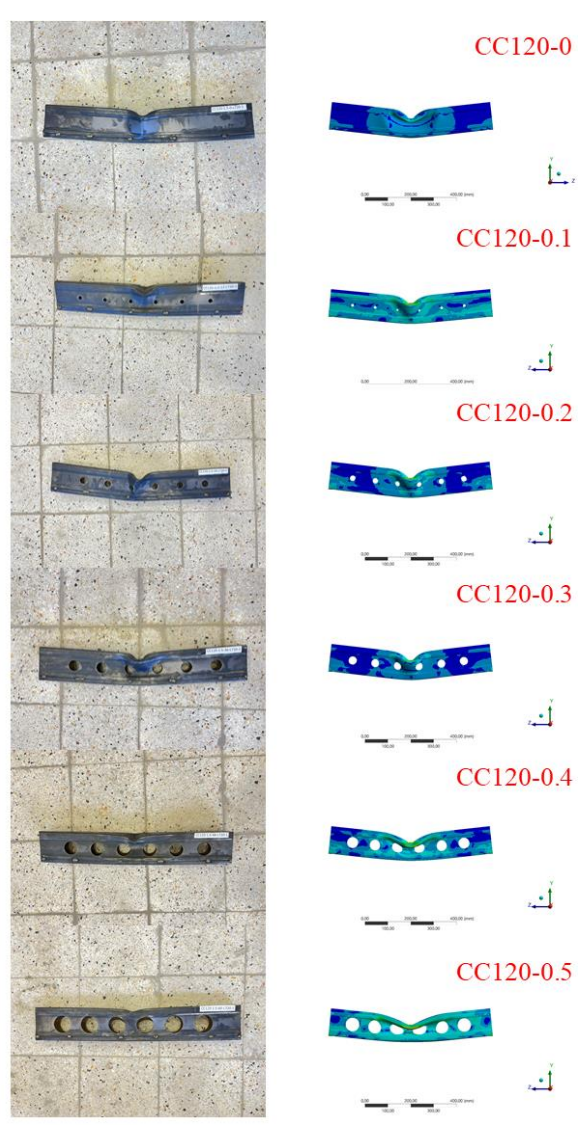


Fig. 7. Comparative analysis of experimental and numerical failure modes

4.3. Ultimate bearing capacity

The ultimate bearing capacity of all specimens in the test is listed in Table 3. The variation of the ultimate bearing capacity with the hole depth-to-web height ratio (dh/h) is shown in Fig. 8. The reduction coefficient of ultimate bearing capacity on the vertical axis in Fig. 7 is based on the non-opening specimen with the same shear-span ratio, as shown in Table 3.

Fig. 7 shows that with a constant web height-to-thickness ratio, larger hole sizes result in smaller ultimate bearing capacities. When the hole depth-to-web height ratio increases from 0 to 0.5, the ultimate bearing capacity decreases from approximately 19% (21.1 kN to 17.1 kN). Smaller shear-span ratios are more sensitive to hole size. As the hole size increases, the ultimate bearing capacity weakens.

The load-deflection curves for specimen CC120 in Fig. 6 show that the ultimate bearing capacity decreases as dh/h increases. When $dh/h \le 0.4$, the curves decrease rapidly after the peak; when dh/h = 0.5, the decrease is more gradual. Mid-span deflection decreases as dh/h increases, showing significant variation for smaller dh/h ratios and stabilizing for dh/h = 0.5.

4.4. Influence of web height-to-thickness ratio

The hole depth-to-web height ratio significantly impacts the shear performance of steel beams. The curves of the ultimate bearing capacity of web-perforated cold-formed C-section steel beams with varying hole depth-to-web height ratios are shown in Fig. 7. It can be seen from the figure that the ultimate bearing capacity of steel beams decreases as the hole depth-to-web height ratio increases. The influence of the hole depth-to-web height ratio on the ultimate bearing capacity of steel beams with $dh/h \le 0.50$ is particularly notable.

When the hole depth-to-web height ratio is small $(dh/h \le 0.4)$, the load-deflection curves at mid-span decrease rapidly after reaching the peak point. Conversely, when the hole depth-to-web height ratio equals 0.5 (dh/h = 0.5), the curves gradually decrease after reaching the peak point. Therefore, the hole depth-to-web height ratio significantly affects the steel beam's ultimate bearing capacity and failure mode.

Table	3	Test	and	FFΛ	results
Tanie	_	1681	аши	FF.A	resillis

Specimen	Ultimate bearing capacity (kN)	Average bearing capacity (kN)	Finite element results (kN)	Estimation error for (%)	
CC120-0-1	21.82	21.11	22.07	4.58	
CC120-0-2	20.39	21.11	22.07	4.38	
CC120-0.1-1	21.38	21.29	21.87	2.73	
CC120-0.1-2	21.20	21.29	21.87	2.73	
CC120-0.2-1	20.65	20.80	20.07	-3.54	
CC120-0.2-2	20.96	20.80	20.07	-3.34	
CC120-0.3-1	18.85	19.09	18.81	-1.52	
CC120-0.3-2	19.34	19.09	16.61	-1.52	
CC120-0.4-1	18.28	18.17	18.29	0.67	
CC120-0.4-2	18.05	16.17	18.29	0.67	
CC120-0.5-1	17.50	17.16	17.00	-0.51	
CC120-0.5-2	16.83	17.10	17.08	-0.31	

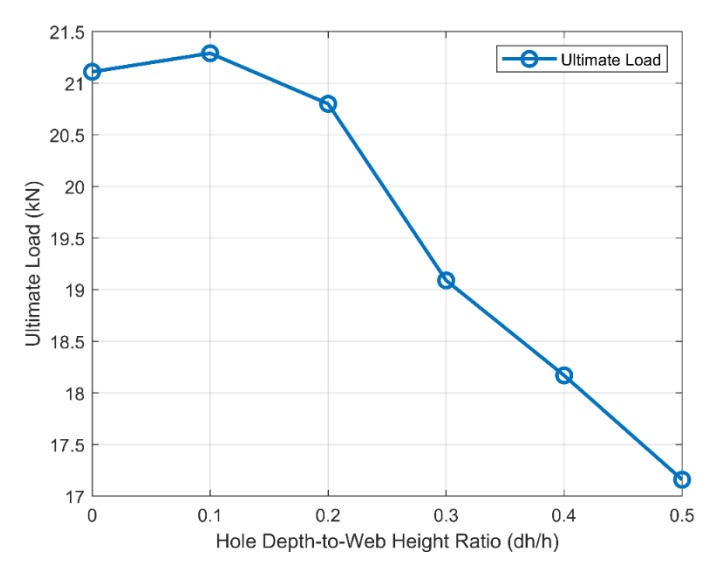


Fig. 8. Relation of ultimate bearing capacity to the hole depth-to-web height ratio

5. Conclusions

This study conducted shear tests on 12 groups of cold-formed C-section steel beams with web openings within the shear span. The finite element models of the specimens were developed using ANSYS, and comparative analysis was performed to validate the models' accuracy. After validating the model, the shear behavior of the specimens was analyzed based on three parameters: the shear-span ratio, the hole depth-to-web height ratio, and the web height-to-thickness ratio. The study led to the following conclusions:

- 1. For a shear-span ratio of 1.5, the stiffness of the steel beams decreases, and the stress concentration area in the web of beams with smaller openings decreases, while the failure mode of beams with larger openings remains relatively unchanged. The failure mode transitions from shear failure to a combination of bending and shear failure as the hole depth-to-web height ratio decreases.
- 2. When the failure mode of the steel beam is primarily shear failure, an increase in the hole depth-to-web height ratio results in a significant reduction in the ultimate bearing capacity of the steel beam. As this ratio increases, failures are predominantly located in the web within the shear span. For a hole depth-to-web height ratio dh/h ≤ 0.4, brittle failure is observed in the steel beams. When the hole depth-to-web height ratio dh/h = 0.5, the beams exhibit some ductility after reaching the ultimate load.
- 3. When the steel beam is mainly subjected to shear failure and its hole depth-to-web height ratio *dh/h* ≤ 0.50, the web height-to-thickness ratio significantly influences the ultimate bearing capacity of the steel beams. However, the web height-to-thickness ratio has a relatively minor effect on the failure mode and stiffness of the steel beams.

In conclusion, this study provides valuable insights into the shear behavior of cold-formed steel beams with web openings, particularly highlighting the significant impact of hole depth-to-web height ratio on ultimate bearing capacity and failure modes. The observed transition from predominantly bending failure to shear failure as hole size increases offers important considerations for structural design. Our experimental results demonstrate the complex relationship between hole size, load-carrying capacity, and ductility in these structural elements. Future work should focus on expanding the range of tested parameters, including investigating the effects of different hole shapes, multiple hole configurations, and varying loading conditions. This would further enhance our understanding of these structural elements under diverse

scenarios. Additionally, exploring the behavior of these beams under dynamic and cyclic loading could provide crucial insights for seismic design applications.

Conflict of interests

The author(s) declared no potential conflicts of interest with respect to the research, authorship, and/or publication of this article.

Funding

This research received no external funding.

Data availability statement

Data generated during the current study are available from the corresponding author upon reasonable request.

References

- [1] Yuan W, Yu N, Li L (2017) Distortional buckling of perforated cold-formed steel channel-section beams with circular holes in web. Int J Mech Sci 126:255–260. https://doi.org/10.1016/J.IJMECSCI.2017.04.001
- [2] Yazici C, Arik E, Özkal FM (2023) Influence of design parameters on beam-to-column connections of steel storage rack systems. Eng Fail Anal 152:107439. https://doi.org/10.1016/J.ENGFAILANAL.2023.107439
- [3] Keerthan P, Mahendran (2014) Improved shear design rules for lipped channel beams with web openings. J Constr Steel Res 97:127–142. https://doi.org/10.1016/j.jcsr.2014.01.011
- [4] Dubina D, Ungureanu V, Gîlia L (2015) Experimental investigations of cold-formed steel beams of corrugated web and built-up section for flanges. Thin-Walled Struct 90:159–170. https://doi.org/10.1016/J.TWS.2015.01.018
- [5] Pham S H, Pham C H, Rogers C A, Hancock G J (2019) Experimental validation of the Direct Strength Method for shear spans with high aspect ratios. J Constr Steel Res 157:143–150. https://doi.org/10.1016/j.jcsr.2019.02.018
- [6] Pham CH, Hancock GJ (2009) Shear buckling of thin-walled channel sections. J Constr Steel Res 65(3):578–585. https://doi.org/10.1016/j.jcsr.2008.05.015
- [7] Degtyarev VV, Degtyareva NV (2016) Finite element modeling of cold-formed steel channels with solid and slotted webs in shear. Thin-Walled Struct 103:183–198. https://doi.org/10.1016/j.tws.2016.02.016
- [8] Degtyarev VV, Degtyareva NV (2017) Numerical simulations on cold-formed steel channels with flat slotted webs in shear. Part II: Ultimate shear strength. Thin-Walled Struct 119:211–223. https://doi.org/10.1016/j.tws.2017.05.028
- [9] Degtyareva NV, Degtyarev VV (2016) Experimental investigation of cold-formed steel channels with slotted webs in shear. Thin-Walled Struct 102:30–42. https://doi.org/10.1016/j.tws.2016.01.012
- [10] Degtyareva N, Gatheeshgar P, Poologanathan K, Gunalan S, Shyha I, McIntosh A (2020) Local buckling strength and design of cold-formed steel beams with slotted perforations. Thin-Walled Struct 156. https://doi.org/10.1016/j.tws.2020.106951
- [11] Degtyarev VV, Degtyareva NV (2018) Numerical simulations on cold-formed steel channels with longitudinally stiffened slotted webs in shear. Thin-Walled Struct 129:429–456. https://doi.org/10.1016/j.tws.2018.05.001
- [12] Degtyareva N, Gatheeshgar P, Poologanathan K, Gunalan S, Tsavdaridis KD, Napper S (2020) New distortional buckling design rules for slotted perforated cold-formed steel beams. J Constr Steel Res 168. https://doi.org/10.1016/j.jcsr.2020.106006
- [13] Thirunavukkarasu K, Kanthasamy E, Poologanathan K, Tsavdaridis KD, Gatheeshgar P, Hareindirasarma S, McIntosh A (2022) Shear performance of SupaCee sections with openings: Numerical studies. J Constr Steel Res 190. https://doi.org/10.1016/j.jcsr.2022.107142
- [14] Laím L, Rodrigues JPC, Da Silva L S (2013) Experimental and numerical analysis on the structural behaviour of cold-formed steel beams. Thin-Walled Struct 72:1–13. https://doi.org/10.1016/j.tws.2013.06.008
- [15] Laím L, Rodrigues JPC, Craveiro HD (2015) Flexural behaviour of beams made of cold-formed steel sigma-shaped sections at ambient and fire conditions. Thin-Walled Struct 87:53–65. https://doi.org/10.1016/j.tws.2014.11.004

[16] Laím L, Rodrigues JPC (2016) Numerical analysis on axially-and-rotationally restrained cold-formed steel beams subjected to fire. Thin-Walled Struct 104:1–16. https://doi.org/10.1016/j.tws.2016.03.004

[17] Živaljević V, Jovanović Đ, Kovačević D, Džolev I (2022) The influence of web holes on the behaviour of cold-formed steel members: a review. Buildings 12(8). https://doi.org/10.3390/buildings12081091